Polyamide 66/poly(2,6-dimethyl-1,4-phenylene oxide) compatibilization with styrene–acrylonitrile–glycidyl methacrylate: rheology, morphology, and mechanical properties

Yun Zhang

zhangyun@ayit.edu.cn

Anyang Institute of Technology

Xinyu Dai

Anyang Institute of Technology

Di Yang

Anyang Institute of Technology

Shaohui Guo

Anyang Institute of Technology

Jinming Yang

Anyang Institute of Technology

Dayong Tian

Anyang Institute of Technology

Kai Wang

Anyang Institute of Technology

Research Article

Keywords: Compatibilization, polyamide 66/poly(2,6-dimethyl-1,4-phenylene oxide) (PA66/PPO), rheology, morphology, styrene–acrylonitrile–glycidyl methacrylate (SAG)

Posted Date: June 30th, 2023

DOI: https://doi.org/10.21203/rs.3.rs-3118184/v1

Additional Declarations: No competing interests reported.

Version of Record: A version of this preprint was published at International Journal of Polymer Analysis and Characterization on February 29th, 2024. See the published version at https://doi.org/10.1080/1023666X.2024.2318518.

Polyamide 66/poly(2,6-dimethyl-1,4-phenylene oxide) compatibilization with styrene–acrylonitrile–glycidyl methacrylate: rheology, morphology, and mechanical properties

Yun Zhang[1], Xinyu Dai[1], Di Yang[1], Shaohui Guo[1], Jinming Yang[1],Dayong Tian[1],Kai Wang[1]

1 College of Chemical and Environmental Engineering， Anyang Institute of Technology, Anyang 455000, China

Correspondence

Yun Zhang，College of Chemical and Environmental Engineering，Anyang Institute of Technology, Anyang 455000, China.

E-mail: zhangyun@ayit.edu.cn

Funding information

Acknowledgement：

Henan Province Key Research and Development Program of China (No.222102230063), Key scientific research projects of colleges and universities in Henan Province (No.22B430001) and Anyang science and technology plan project (No.2021C01GX003)

Abstract

During the blending process, Styrene–acrylonitrile–glycidyl methacrylate (SAG) was grafted through in-situ formation of PA66 as a compatibilizer for polyamide 66/poly (2,6-dimethyl-1,4-phenoxy) (PA66/PPO) composites. The compatibilizer has a obvious advantage on the PA66/PPO blends terminal behavior in the dynamic rheological analysis. Moreover, the gap between the PA66 and PPO glass-transition temperatures decreases with the SAG content increasing, which indicates improved compatibility. The morphology of the PA66/PPO/SAG blends was analyzed by scanning electron microscopy, which revealed the particles narrower size distributions and became smaller after adding SAG. In addition, the compatibilization improves the mechanical properties of blends significantly when SAG reached 5 by weight per

hundred resins (phr). This is attributed to enhanced interfacial adhesion and finer dispersion morphology. However, when 7 phr of SAG are added, the exceeded compatibilizer produces a limitation on the improvement of the mechanical properties. Our results indicate that the optimal concentration of the compatibilizer, SAG, is between 3 and 5 phr for PA66/PPO (60/40).

HIGHLIGHTS

- SAG was confirmed to be an efficient reactive compatibilizer for PA66/PPO blends.
- The viscoelastic properties of compatibilized changed by the in-situ reaction.
- The mechanical properties improved significantly after adding SAG.

KEYWORDS

Compatibilization, polyamide 66/poly(2,6-dimethyl-1,4-phenylene oxide) (PA66/PPO), rheology, morphology, styrene–acrylonitrile–glycidyl methacrylate (SAG)

1 INTRODUCTION

Polymer blending is an effective way to develop new materials with improved properties. Polyamide 66/poly(2,6-dimethyl-1,4-phenylene oxide) (PA66/PPO) is a representative blend, for which PPO adds higher dimensional stability and better thermal properties, while PA66 improved chemical resistance and processability. Given their inherent properties, the combination of PPO with PA66 is expected to reduce their defects. [1–5] Unfortunately, PA66 and PPO are immiscible polymers due to the large polarity differences and high interfacial tension. Simply melting PPO compounded with PA66 lead to poor mechanical properties since the bad interfacial adhesion and relatively low toughness of both phases. [6–10] Therefore, compatibilization is required to obtain good PA66/PPO blends. Successful compatibilization would also aid the development of improved blending modification methods.

Many studies of compatibilization of PA/PPO blends have been carried out over the last few decades. The compatibilizer is an effective approach to enhance the compatibility of PA/PPO blends because blocks of grafted copolymers show intermolecular interactions with both components. Typically, copolymers including glycidyl methacrylate (GMA) or maleic anhydride (MA) were added into PA/PPO blends as compatibilizer. [11–14] Polystyrene-grafted maleic anhydride (SMA) is a typical compatibilizer for PA/PPO blends because the anhydride group can react with the amine group of PA6, and styrene segments are miscible with PPO. [15] Thus, *in-situ* formed PA-g-SMA could increase the interfacial adhesion and successfully decrease the particle sizes in dispersed phase. [16-18] Moreover, functional PPO also a typical of modifier used to compatibilize PA/PPO blends. The addition of PPO-g-MA can avoid the domains coalescence dispersed, and achieve a uniform morphology. [19-20]

In the paper, styrene–acrylonitrile–glycidyl methacrylate (SAG, denoted as SAG) was used to compatibilize PA66/PPO blends. Here, epoxy groups of GMA can react with amine or carboxyl end-groups of PA66, and form an *in-situ* copolymer, PA66-*graft*-SAG. In addition, it will also interact with PPO, and the styrene segment is miscible with PPO phase. As reported, both strength and heat resistance of PPO are enhanced efficiently upon addition of SAN. [21] Thus, SAG copolymer will become a fine compatibilizer and raise the mechanical properties of PA66/PPO. The content of SAG on viscoelastic properties, morphology, mechanical, and thermal properties of PA66/PPO blends were investigated. The viscoelastic properties of immiscible blends were researched to illustrate the formation of melt grafted copolymers.

2 EXPERIMENTAL

2.1 Materials

PA66 (EPR27) and PPO (LXR45) were obtained with Shenma Industrial Co. and China National Bluestar Co., respectively. The SAG compatibilizer (grade SAG-005) was acquired with Nantong Sunny polymer New Material Technology Co. Ltd. The melt index of SAG is 8.0 ± 2 g/10 min, and the epoxy group content is 5.0 ± 0.5 wt % (ASTM D1652).

2.2 Sample preparation

The melt compounding of PPO and PA66 blends was processed by a twin-screw extruder. The screw diameter was 25 mm, length-diameter ratio (*L/D*) was 40, speed was settle in at 300 rpm, and barrel temperatures were set between 240 and 285 ºC. The weight ratio between PA66 and PPO was 60/40 (wt. %). The concentrations of SAG were 0, 1, 3, 5, and 7 with parts per hundred resins by weight (phr). The whole materials were dried at 100 ºC for 24 h and premixed for 10 min. The blended pellets were dried in a vacuum oven at 100 ºC for 10 h, and pressed into standard samples by a HAITIAN SA900/260 injection molding machine at the barrel temperatures 270, 280, 285, 290, and 280 ºC with an injection pressure of 60 MPa.

2.3 Characterization

The Fourier transform infrared spectrometer (FTIR) analyses of PA66, PPO, SAG, and PA66/PPO (60/40) blends were carried out using a Thermo Scientific Smart OMNI-Sampler. All samples were mold-pressed into 100-μm-thick films at 280 °C before analysis.

The dynamic rheological was measured by Haake Mars-III rheometer with a parallel-plate (diameter 20 mm and gap 1 mm) mode. The blends dynamic rheological behaviors were recorded at declining frequency from 100 to 0.01 s^{-1} at 280 °C in N_2 atmosphere.

The Hitachi-S4700 scanning electron microscopy (SEM) used to describe blends morphology. The surfaces of samples were etched in chloroform 8 h to dissolve PPO purposively. Subsequently, the etched surfaces were placed in vacuum at 80 °C.

The volume-average particle diameter $\overline{d_v}$ and the-number average particle diameter $\overline{d_n}$ of the dispersed phase were analyzed by image J 1.41and calculated.

$$\overline{d_v} = \frac{\sum N_i d_i^4}{\sum N_i d_i^3} \tag{1}$$

$$\overline{d_n} = \frac{\sum N_i d_i}{\sum N_i} \tag{2}$$

Where N_i is the particles number with diameter d_i. The particles number was 500–6 per sample.

The tensile (ISO-8256-2005) and flexural (ISO-178-2010) properties were obtained by the device (XWW, Chengde Jinjian Testing Instruments Co., Ltd.) at a crosshead speed of 50 mm min^{-1} and 2 mm min^{-1}, respectively. Notched impact strengths (ISO-179-2010) were got by the instrument (ZBC 1400-2, Shenzhen Sans Material Test Instrument Co., Ltd.). The results of five measurements for each sample were averaged.

The dynamic-mechanical thermal properties of PA66/PPO blends were analyzed using a DMA 7E (Perkin Elmer Inc.) with a sample dimension of 35×6×2 mm^3, and the frequency was 1 Hz with a stretching ratio of 0.1 %. The T_g of PA66/PPO/SAG, samples were heated from 20 °C to 250 °C at temperature increasing rate of 5 °C/min.

3 RESULTS AND DISCUSSION

3.1 FTIR analysis

The GMA epoxy groups can in situ-reacted with amine or carboxyl end-groups of PA66.

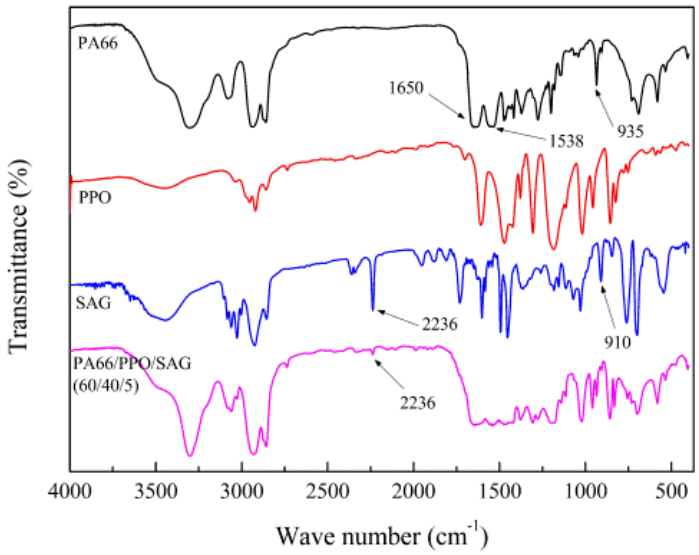

FIGURE 1 The FTIR spectra of PA66, PPO, SAG, and PA66/PPO/SAG (60/40/5)

To study the compatibilization mechanism of SAG further, the FTIR spectra of

PA66, PPO, SAG, and PA66/PPO/SAG (60/40/5) were recorded – see Figure 1. For pristine PA66, the absorption bands at 1650 and 1538 cm^{-1} correspond to carbonyl stretching ($\nu_{C=O}$) and N–H bending (ν_{N-H}), respectively. Most bands were shielded by the added PPO. The SAG spectra show a peak for the nitrile group at 2240 cm^{-1}, which corresponds to $\nu_{N\equiv H}$ stretching. The epoxy group of SAG produces a characteristic absorption band at 910 cm^{-1}. The band at 2240 cm^{-1} was observed after the addition of SAG in the PA66/PPO blends. The weak epoxy peak at 910 cm^{-1} disappeared after extrusion, which indicates that a reaction between SAG and the end-groups of PA66 has occurred.

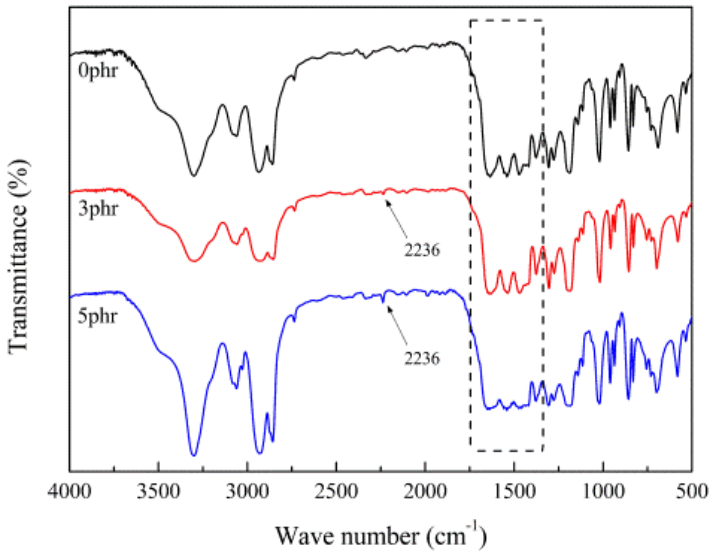

FIGURE 2 The transmission spectra of the PA66/PPO blends with different SAG content

The transmission spectra of the PA66/PPO blends with different SAG content are shown in Figure 2. The characteristic peak at 2240 cm^{-1} of the nitrile group was used to monitor the addition of SAG. The band at 2240 cm^{-1} emerged clearly with increasing SAG content. The epoxy peak at 910 cannot be observed in compatibilized samples, probably because it was completely consumed by the above-mentioned reactions. Moreover, the bands for carbonyl stretching ($\nu_{C=O}$) and N–H bending (ν_{N-H}) became less sharp and merged together upon adding SAG, which indicates that the characteristic peaks are affected by *in-situ* reactions in blends.

3.2 Rheology of the PA66/PPO blends

The viscoelastic properties of polymers are sensitive to changes in the molecular structure and phase morphology of the blends [22]. Therefore, the dynamic rheology of blends was analyzed to investigate the compatibilization effect of SAG.

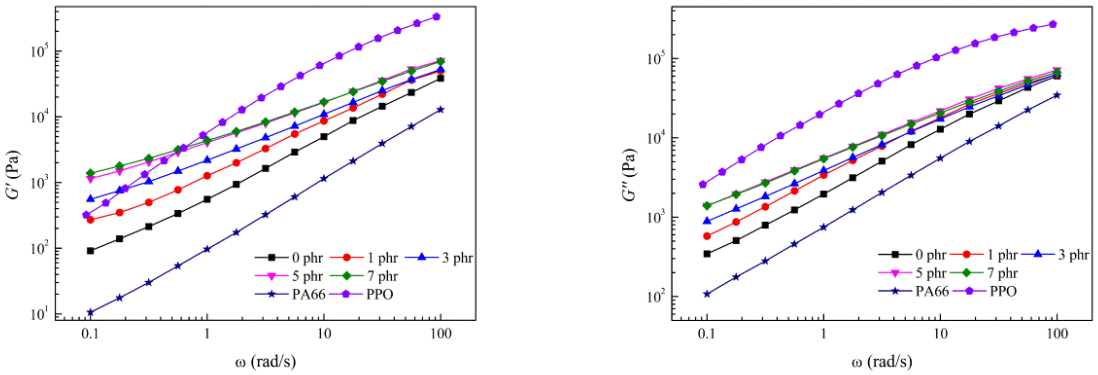

(a) G’ (b) G”

FIGURE 3 The storage modulus (G’) and loss modulus (G”) of the PA66/PPO blends with different SAG content

Table 1 Rheological parameters of PA66, PPO, and compatibilized PA66/PPO blends

Content of SAG	PA66	PPO	0 phr	1 phr	3 phr	5 phr	7 phr
Terminal slope of *G’*	0.77	1.21	0.65	0.53	0.53	0.51	0.45
Terminal slope of *G’’*	0.83	0.94	0.74	0.72	0.63	0.59	0.57

The storage modulus (*G’*) of the PA66/PPO blends with different SAG content plotted as a function of frequency are shown in Figure 3(a). The *G’* increases with increasing SAG content. In the terminal zone, the slope of *G’* directly reflects the relaxation of macromolecular chains in the blends. The pristine PPO and PA66 show typical terminal behavior, where the slope of *G’* is near 2.[23] With the addition of SAG, the terminal slope of *G’* decreases and *G’* increases significantly (Table 1). This suggests a longer lasting relaxation mechanism, which can improve the interfacial

adhesion caused by the in-situ formation of a copolymer. Thus, a longer relaxation time is required because of increasing interaction between the PPO and PA66 chains. For blends with a SAG content of 7 phr, the increase of *G'* at low frequency was not significant, which indicates that increasing the amount of compatibilizer has little effect on the terminal behavior when the SAG content exceeds 5 phr. This may be due to the interface of PA66/PPO being saturated with the PA66-*graft*-SAG copolymers. The loss modulus (*G"*) of the PA66/PPO blends with different SAG content, plotted as a function of frequency, shown in Figure 3(b). The pristine PPO and PA66 exhibit typical terminal behavior, where the slope of *G"* is closer to 1. The *G"* of blends with added SAG shows similar terminal behavior as the *G'* results at low frequency, which suggests improved interfacial adhesion.

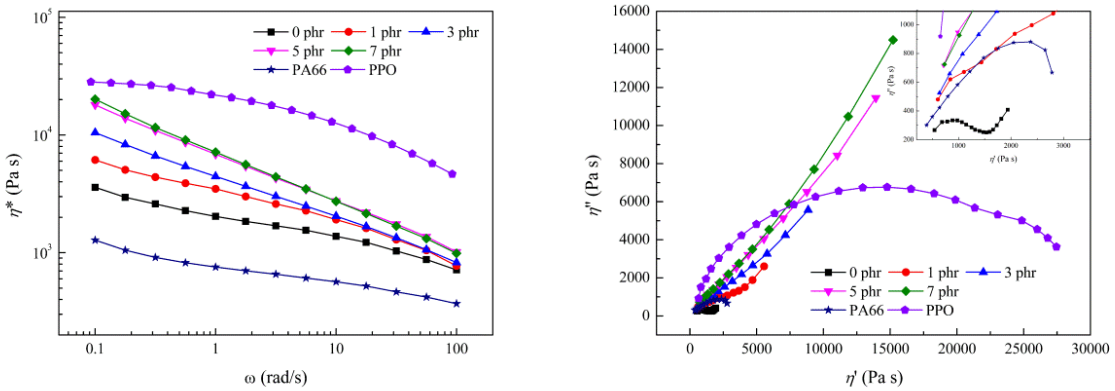

(a) Complex viscosity (b) Cole-Cole plot

FIGURE 4 The complex viscosity and Cole-Cole plot of the PA66/PPO blends with different SAG content

Figure 4(a) illustrates the complex viscosity of the PA66/PPO blends with different SAG content as a function of frequency. Consistent with the variation of the storage modulus, the complex viscosity increases significantly after adding SAG, except for SAG loading of 7 phr. According to the literature, the complex viscosity of blends is sensitive to the interaction provoked by the presence of the functional group and/or the formation of a new copolymer, especially at low frequencies. [24, 25] Moreover, the enhanced interfacial adhesion can improve the dispersion morphology

that causes increased interfacial friction. However, the complex viscosity did not increase significantly for high SAG loading (7 phr). This may be due to two reasons: (a) the excess SAG acts as a plasticizer for PPO phase (b) the morphological structure of the blends is affected by the reaction between compatibilizer and PPO, which discussed at the following section.

Phase separation in modified blends can be visualized in the Cole-Cole plot (η''-η'). The Cole-Cole plots of pristine PA66, pristine PPO, and PA66/PPO blends with different SAG content are shown in Figure 4(b). For the pristine PA66 and PPO, the curves resemble a semicircle. The higher the molecular weight is, the bigger the radius becomes. For the binary PA66/PPO blends, a tail appears on the right side of the circular arc at high viscosity, which clearly suggests phase separation. The curves for the PA66/PPO blends with added SAG have a higher radius than for the binary blends. This can be attributed to a longer relaxation time. The upturning tail of the curves weakens with increasing SAG concentration, which indicates that the interfacial adhesion improved.

3.3 Morphology

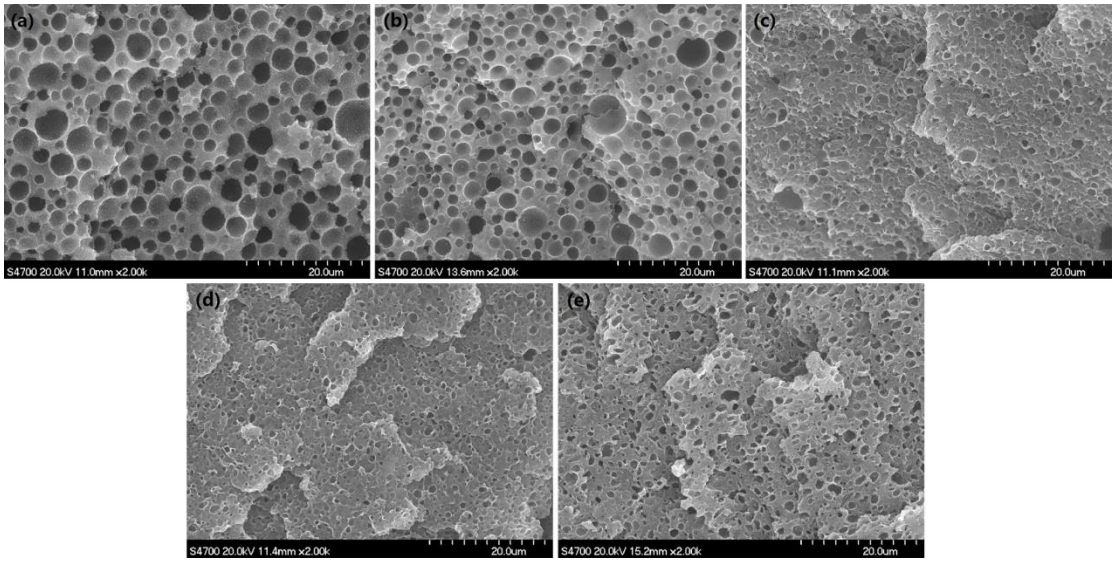

FIGURE 5 The phase morphology of the PA66/PPO blends (a) 0 phr (b) 1 phr (c) 3 phr (d) 5 phr and (e) 7 phr

To investigate the compatibilization effect of SAG in more detail, the PA66/PPO

blends morphology was observed by SEM – see Figure 5. The cavities in the micrographs indicate the presence of a PPO phase, and the continuous phase is PA66 with its lower viscosity. Because of the high interface tension and poor compatibility, the binary blends show poor dispersion of the PPO phase with large particle sizes and a broad size distribution – see Figure 5(a). However, with the addition of SAG, the diameter of PPO domains decreased significantly – see Figure 5 (b-e).The particle size of the PA66/PPO blend with only 3 phr of SAG decreased to about one-third of the un-compatibilized blend. The particle size distributions of all samples are shown in Figure 6. A narrower size distribution was obtained with increasing SAG loading, which indicates a uniform scale of the dispersed phase. The smaller particles indicate a higher interphase amount, which results in increased viscosity. However, when the SAG content exceeds 5 phr, the morphology of PPO domains are less dependent on compatibilizer loading.

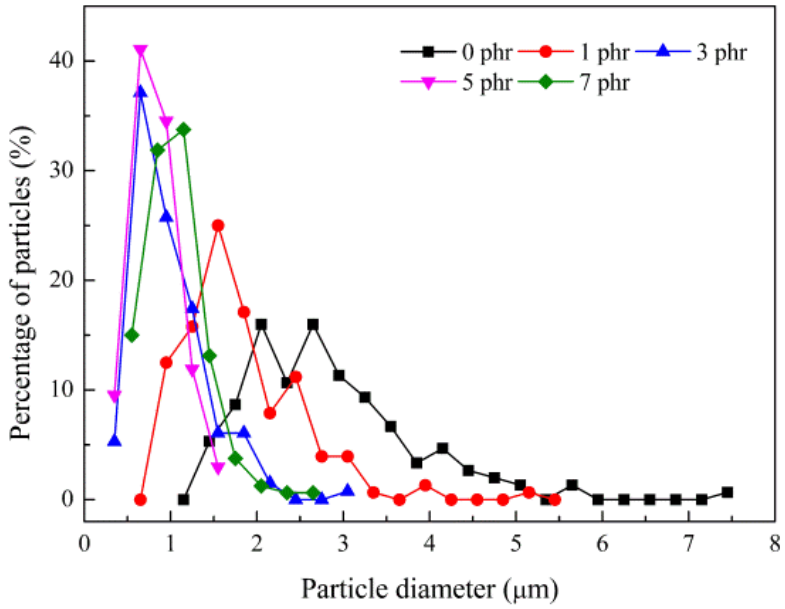

FIGURE 6 The particle size distributions of all samples by different speeds

Table 2 The data of DMTA for PA66/PPO (60/40) blends

SAG Content (phr)	0	1	3	5	7

d_v (μm)	4.01	2.73	1.65	1.05	1.5

When observing the PPO/PA66 blends at high magnification (Figure 7), a clear and regular interface is visible in the blends without compatibilizer, which is attributed to poor interfacial adhesion. Upon increasing the content of SAG, the shape of the PPO domains becomes more irregular and less clearly defined interfaces are obtained. For the blends with 5 and 7 phr SAG, small granules were observed on the surface of cavities, which is probably due to unreacted SAG – see black circles in Figure 7(d, e). As shown in Table 2, the particle size does not decrease further when the content of SAG exceeds 5 phr. These indicate that the *in-situ* formed copolymer significantly improves the compatibility of PA66/PPO blends; however, the interface of blends could be saturated by the copolymer at high SAG content (7 phr).

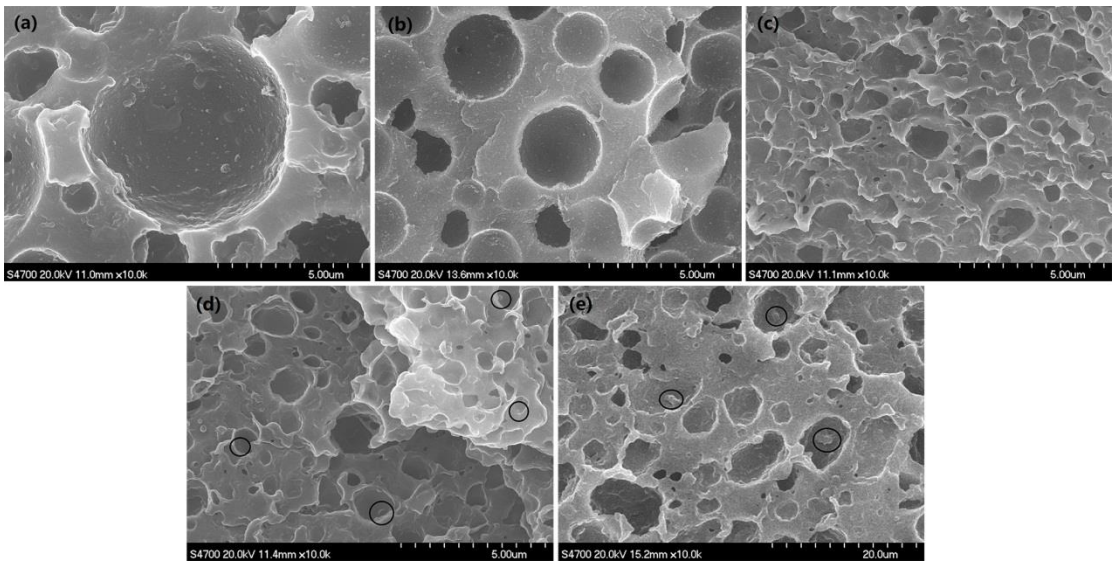

FIGURE 7 The PPO/PA66 blends observe by SEM at different speeds (a) 0 phr (b) 1 phr (c) 3 phr (d) 5 phr and (e) 7 phr

3.4 Mechanical properties

The morphological structures and interfacial adhesion impact on mechanical properties of immiscible blends. Figure 8(a) demonstrates the impact strength and elongation at break of PA66/PPO for different SAG contents. The toughness was improved significantly by SAG. The notched impact-strength increased from 2.8 to

8.5 kJ/m^2 when the loading of SAG increased to 5 phr. Meanwhile, the elongation curve at the break reveals a similar trend for the impact strength of blends, which indicates higher toughness. These phenomena are attributed to the *in-situ* formed copolymer compatibilization effect. Moreover, the finer dispersion morphology results in more crazes during mechanical tests, which absorb the impact energy. However, a decrease in impact strength was observed when 7 phr of SAG was added. According to the literatures, the decrease can be ascribed to the reaction between too much SAG and the PPO phase, which reduces the toughness of the dispersion.

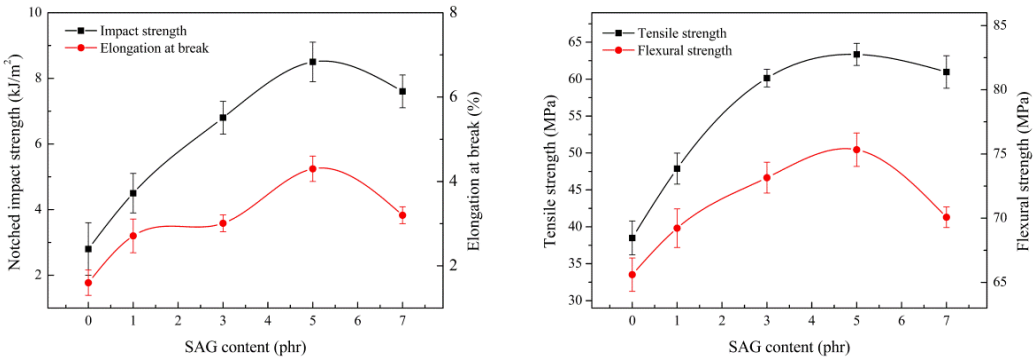

(a) impact strength and elongation

(b) The tensile and flexural strength

FIGURE 8 The impact strength, elongation, tensile and flexural strength at break of PA66/PPO blends for different SAG contents

The tensile and flexural strength of the PA66/PPO (60/40, wt. %) blends are shown in Figure 8(b). For blends without compatibilizer, the large dispersed particles and phase separation would induce defects and stress concentration during the test. The tensile strength increased from 38.5 to 60.1 MPa after the addition of only 3 phr SAG. When the content of SAG exceeded 5 phr, we observe no further improvement for both tensile strength and flexural strength, probably due to the plasticizer effect. Considering the morphological and mechanical improvements, we can confirm that SAG is an effective compatibilizer for PA66/PPO blends.

3.5 Dynamic mechanical thermal analysis (DMTA)

Table 3 The data of DMTA for PA66/PPO (60/40) blends

SAG content (phr)	T_g (ºC)		E' (Mpa, 30 ºC)	E' (Mpa, 150 ºC)
	PA66	PPO		
0	67.10	213.35	976.0	526.04
1	68.45	212.34	1062.8	509.74
3	73.07	211.47	1149.5	487.68
5	75.14	209.35	1163.0	482.96
7	71.08	208.05	1109.2	446.65

For reactive compatibilized blends, the glass transition temperature (T_g) and modulus are directly related to the reactions and phase morphology. Thus, the dynamic mechanical and thermal properties of PA66/PPO were further investigated to evaluate the compatibilization effect of SAG. Figure 9(a) illustrates the plots of the loss tangent (tan δ) versus temperature of binary and compatibilized PA66/PPO blends. The melting temperature of PA66 (260 °C) was reported to have a large difference compared to the T_g of PPO (210°C). Thus, the peaks in the plot correspond to the T_g of PA66 and PPO. The PA66/PPO blend without SAG shows a T_g PA66 (67.1 °C) and PPO (213.35 °C)-see Table 3. Clearly, the ΔT_g decreases with increasing loading of SAG. This indicates the compatibility of the PA66/PPO has an improvement. When the content of SAG exceeds 3 phr, a minor peak appears at 120 °C. We suspect that the presence of the minor peak is caused by the in-situ formed PA66-*graft*-SAG copolymer.

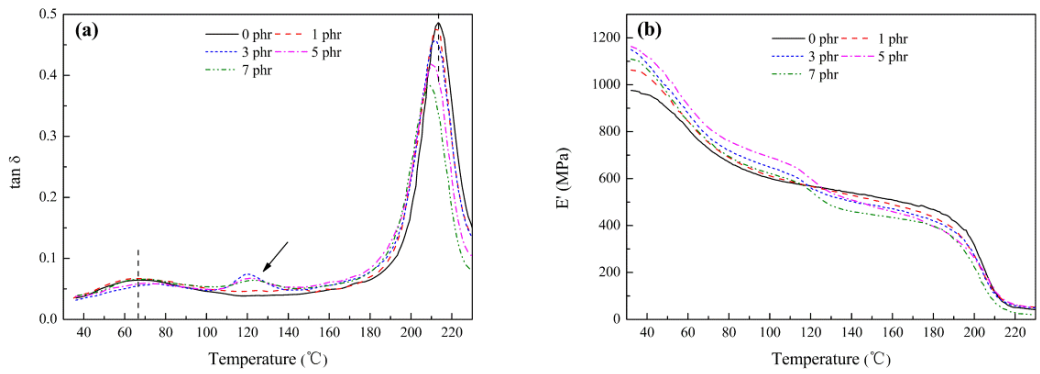

(a) Dynamic mechanical and thermal (b) Storage modulus

FIGURE 9 The dynamic mechanical and thermal properties of the PA66/PPO blends

Figure 9(b) is shown the plots of the storage modulus (*E'*) versus temperature for PA66/PPO blends. For all samples, two obvious decreases of *E'* with temperature rising, which correspond to the chain segment relaxation of PA66 and PPO, respectively. The compatibilized blends show a higher *E'* than the binary blends did at low temperatures. This is attributed to enhanced interfacial adhesion, which the rigidity increased. The *E'* of the blends decreases with the addition of SAG in the temperature range 140 to 200 °C, especially for the sample with 7 phr content. This is because SAG could act as a plasticizer for PPO phase, which results in the decrease of the modulus.

4 CONCLUSIONS

In this study, SAG is confirmed that the compatibilizer is efficient for PA66/PPO blends. The epoxy group of SAG can react with the amine and carboxyl end groups of PA66; in addition, the styrene segment is compatible with the PPO phase. The changes in viscoelastic properties of compatibilized blends, such as higher G' and G" at low frequencies, are related to the formation of a copolymer caused by the *in-situ* reaction. The increasingly complex viscosity of blends suggests enhanced interfacial adhesion. The compatibilization effect of SAG further reduces interfacial tension, which leads to improvements in both the morphological and mechanical properties. The dispersion particle size decreases significantly, and the mechanical properties of the blends improve after adding SAG. However, when 7 phr of SAG are added, the interface of the blends is saturated by the copolymer, which imposes a limitation effect on the mechanical properties. Overall, SAG is confirmed as efficient compatibilizer of PA66/PPO. To achieve the best mechanical properties of PA66/PPO (60/40 wt. %), an SAG content of 3 to 5 phr is best.

ACKNOWLEDGMENTS

This work was financially supported by grant from the Henan Province Key Research and Development Program of China (No.222102230063)， Key scientific research projects of colleges and universities in Henan Province (No.22B430001)， Anyang science and technology plan project (No.2021C01GX003) and Henan Province College Student Innovation and Entrepreneurship Training Program Project (No.202311330036)

DATA AVAILABILITY STATEMENT

Data available on request form the authors.

ORCID

Yun Zhang: 0000-0002-6990-269X

REFERENCES

1. Li Y , Xie T , Yang G . Journal of Applied Polymer Science, 2010, 99(1):335-339.

2. Zhang Y T , Li Y , Li L , et al. Key Engineering Materials, 2012, 501.

3. Jana S C , Patel N , Dharaiya D. Polymer, 2001, 42(21):8681-8693.

4. Li Y L , Xie T X , Yang G S. Journal of Applied Polymer Science, 2006(5):99.

5. Liu A , Xie T , Yang G. Macromolecular Chemistry & Physics, 2010, 207.

6. Puskas J E , Kwon Y , Altst?Dt V , et al.. Polymer, 2007, 48(2):590-597.

7. Jana S C , Patel N , Dharaiya D. Polymer, 2001, 42(21):8681-8693.

8. Tol R T , Groeninckx G , Vinckier I , et al. Polymer, 2004, 45(8):2587-2601.

9. Chu P P , Huang J M , Wu H D , et al. Journal of Polymer Science Part B Polymer Physics, 2015, 37(11):1155-1163.

10. Li J , Nagai K , Nakagawa T，et al. Journal of Applied Polymer Science, 2010, 61(13):2467-2470.

11. Wu D , Wang X , Jin R. European Polymer Journal, 2004, 40(6):1223-1232.

12. Bo L , Wan C , Yong Z , et al. Journal of Applied Polymer Science, 2010, 115(6):3385-3392.

13. Chiang C R , Chang F C. Polymer, 1997, 38(19):4807-4817.

14. Guo Z , Yu S , Fang Z. Journal of Polymer Engineering, 2014, 34(2):193-199.

15. Libo, Du, Guisheng, et al. Journal of Applied Polymer Science, 2008, 108(5):3419-3429.

16. Shuai W , Bo L , Yong Z. Journal of Biomedical Materials Research Part B Applied Biomaterials, 2010, 101B(5):3545-3551.

17. Peng H , Lam J , Tang B Z. Macromolecular Rapid Communications, 2010, 26(9):673-677.

18. Sun L, Shi Y, Li B, et al. Polymer Composites, 2013, 34(7): 1076-1080.

19. Hachiya H, Takayama S, Takeda K. Journal of applied polymer science, 1998, 70(12): 2515-2520.

20. Ajji A, Choplin L, Prud'Homme R E. Journal of Polymer Science Part B: Polymer Physics, 1988, 26(11): 2279-2289.

21. Van Ruymbeke E, Stéphenne V, Daoust D, et al. Journal of Rheology, 2005, 49(6): 1503-1520.

22. Marco C, Ellis G, Gómez M A, et al. Journal of applied polymer science, 1997, 65(13): 2665-2677.

23. Leu Y Y, Mohd Ishak Z A, Chow W S. Journal of applied polymer science, 2012, 124(2): 1200-1207.

24. Chiang C R, Chang F C. Journal of applied polymer science, 1996, 61(13): 2411-2421.27.

25. Tian J, Yu W, Zhou C. Polymer, 2006, 47(23): 7962-7969.